

Supporting information

Strong interfacial coupling through exchange interactions in soft/hard core-shell nanoparticles as function of cationic distribution

Kevin Sartori,^{1,2} Geoffrey Cotin,¹ Corinne Bouillet,¹ Valérie Halté,¹ Sylvie Bégin-Colin,¹ Fadi Choueikani,² Benoit P. Pichon^{*,1,3}

¹ Université de Strasbourg, CNRS, Institut de Physique et Chimie des Matériaux de Strasbourg, UMR 7504, F-67000 Strasbourg, France

²Synchrotron SOLEIL, L'Orme des Merisiers, Saint Aubin – BP48, 91192 Gif-sur-Yvette, France

³Institut Universitaire de France, 1 rue Descartes, 75231 Paris Cedex 05

Corresponding Author

E-mail: Benoit.Pichon@unistra.fr

Tel: 0033 (0)3 88 10 71 33, Fax: 0033 (0)3 88 10 72 47

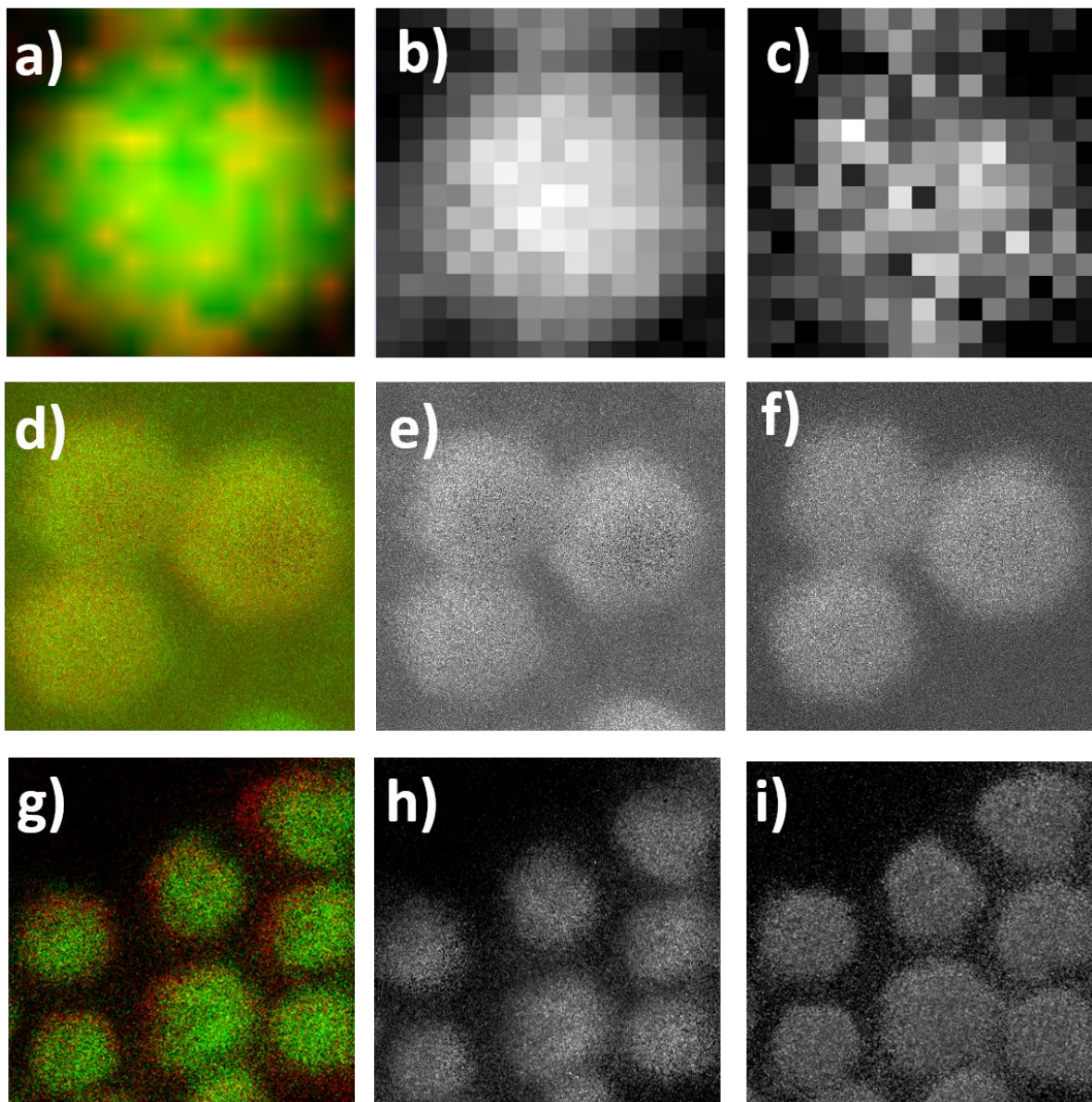


Figure S1. Integrated maps of the element EEL spectra showing Fe and Co distribution. a), d), g) Composite images showing Fe (green) and Co (red), b), e), h) Fe L_{2,3} signal and c), f), i) Co L_{2,3} signal showing the distribution of Fe and Co, respectively, in nanoparticles.

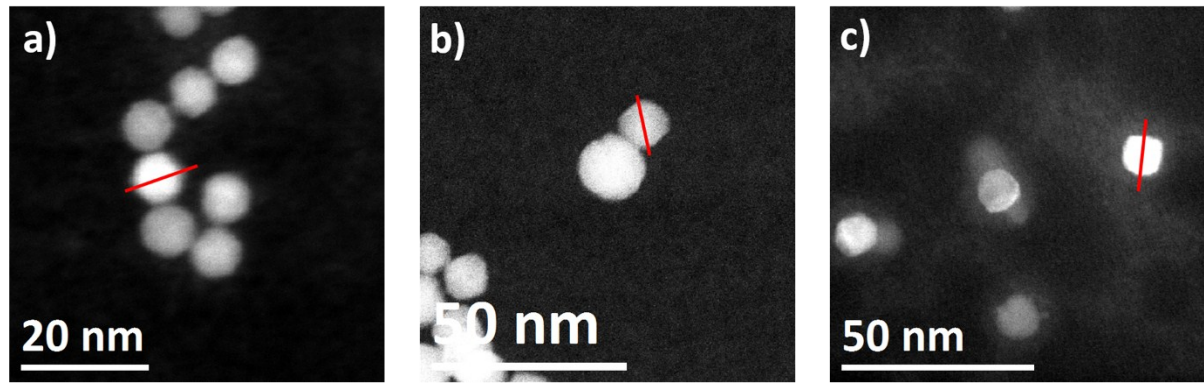


Figure S2. Image spectra of a) CS_CoF1 b) CS_CoF2 c) CS_CoO with red lines corresponding to the EELS profile section shown in Figure 2.

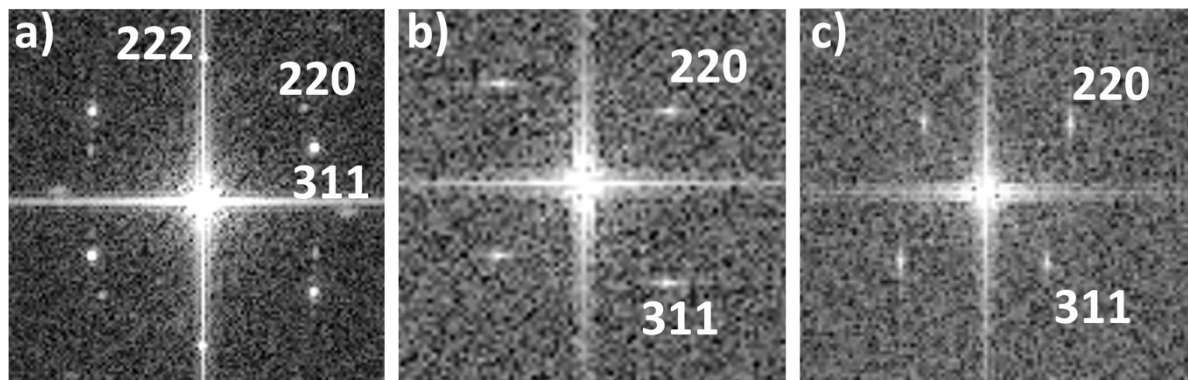


Figure S3. Fast Fourier Transform of HAADF micrographs for a) CS_CoF1, b) CS_CoF2 and c) CS_CoO showing the (hkl) orientations.

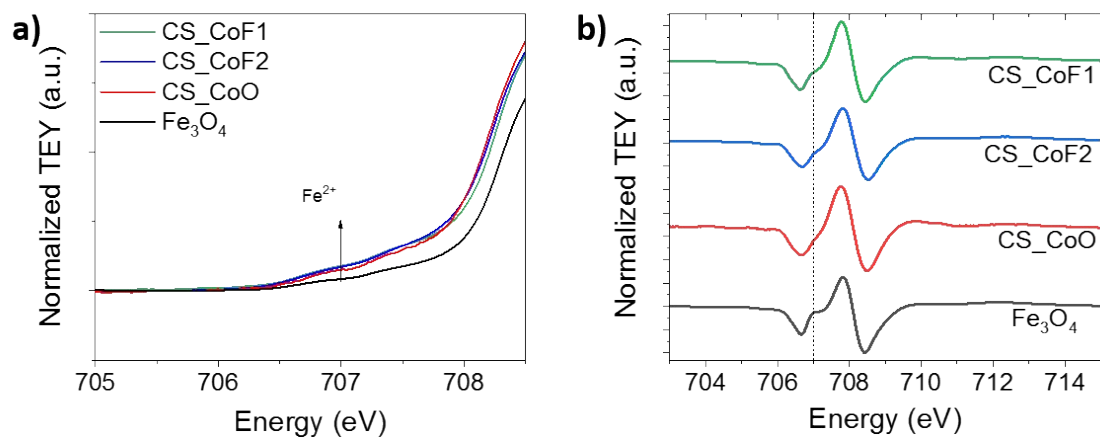


Figure S4. Enlargement of a) XAS and b) XMCD spectra showing the shoulders at 707 eV.

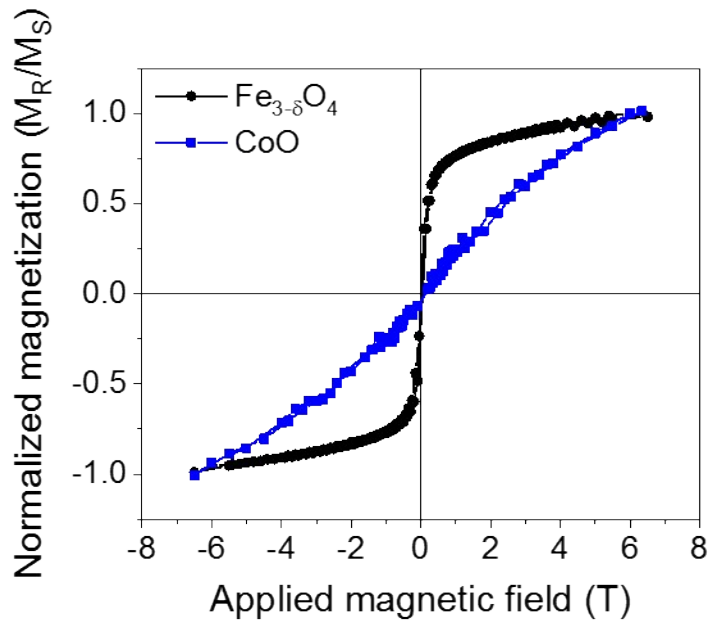


Figure S5. Element specific XMCD $M(H)$ curves recorded at Fe (S1) and Co edges at 4 K for $\text{Fe}_{3-\delta}\text{O}_4$ and CoO nanoparticles.

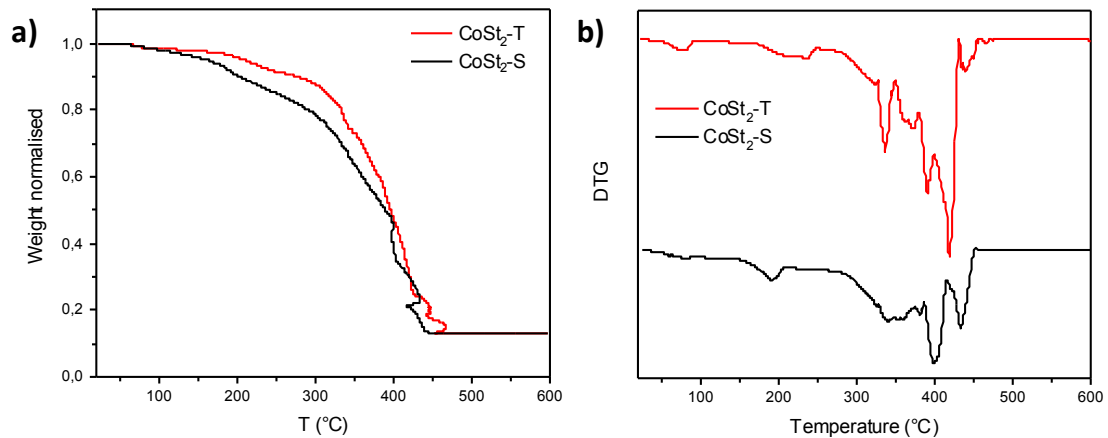


Figure S6. a) Thermogravimetric curves and b) the corresponding thermodifferential curves of cobalt precursors used for the synthesis of core-shell nanoparticles.

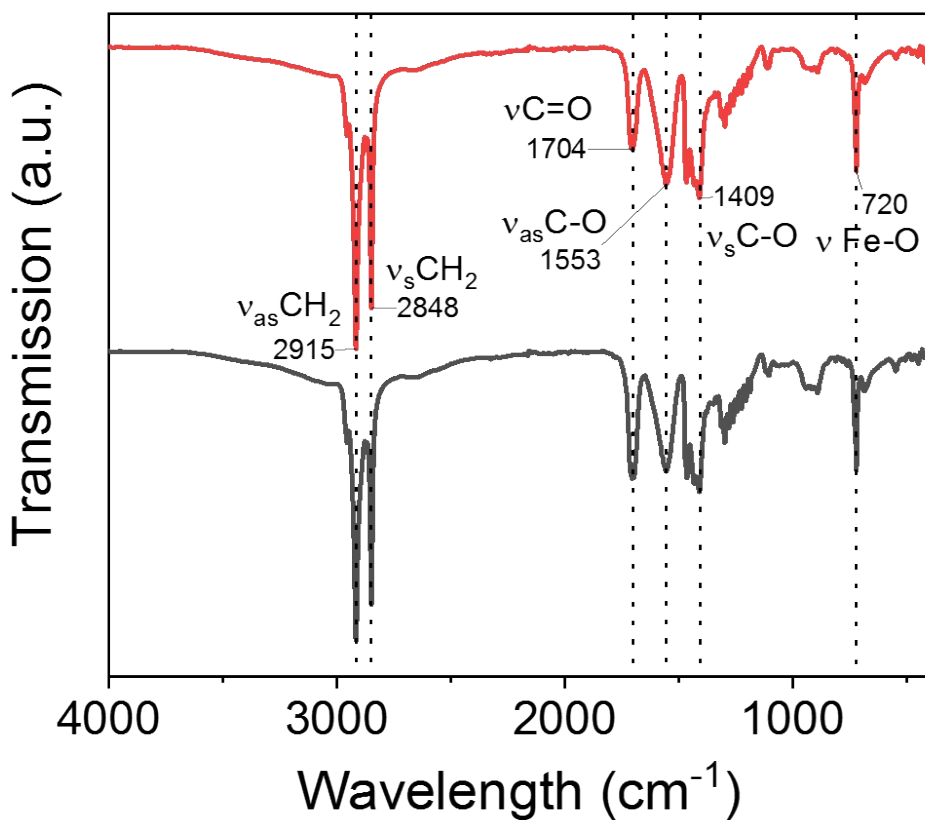


Figure S7. FTIR spectra of Co precursors. CoSt2-T (up) and CoSt2-S (down).

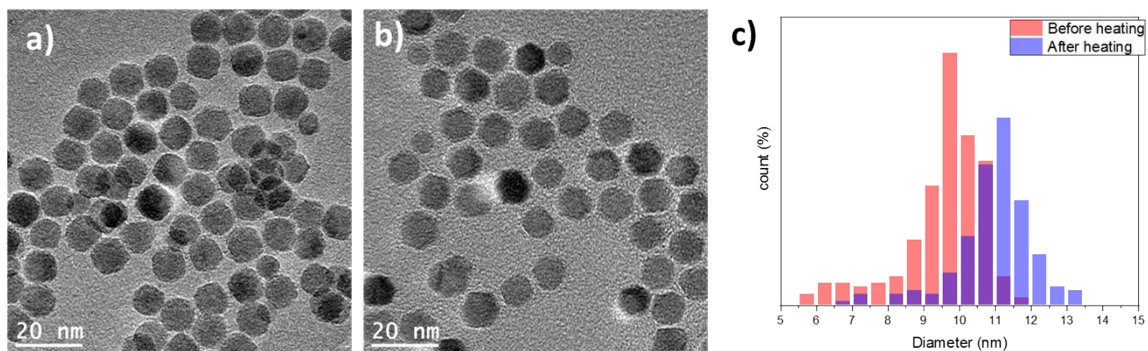


Figure S8. TEM micrographs of iron oxide nanoparticles before (a) and after (b) performing the second heating without any addition of Co precursor in the reaction medium. c) Size distributions measured from TEM micrographs.

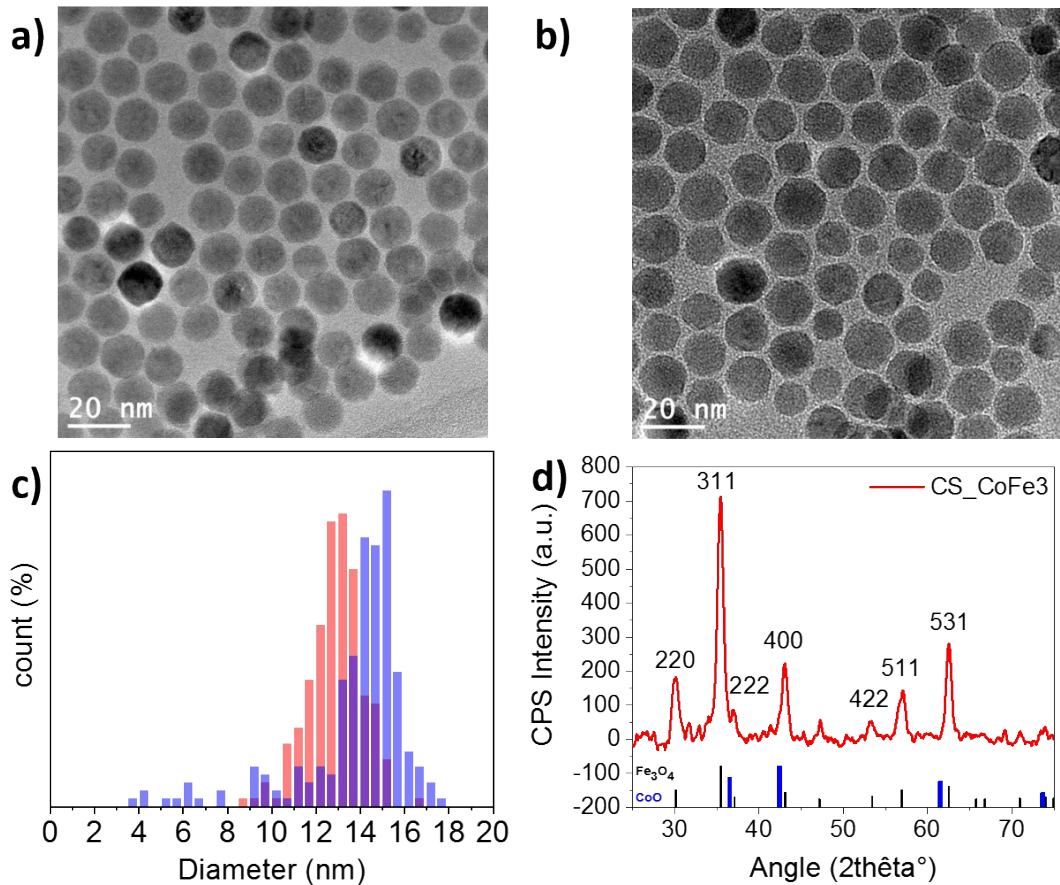


Figure S9. TEM micrographs of (a) pristine iron oxide nanoparticles before and (b) core-shell nanoparticles CS_CoF3 after performing the thermal of CoSt2-T precursor ($R = 2$). c) Size distributions measured from TEM micrographs. d) XRD pattern of core-shell nanoparticles showing the presence of the $\text{Fe}_{3-\delta}\text{O}_4$ spinel phase (black histogram) and wüstite CoO phase (blue histogram).

Nanoparticle	Fe	Co
8	73	27
9	68	32
10	71	29
11	68	32
12	66	34
13	63	37
14	59	41
15	60	40
16	66	34
17	65	35
Average	66	34

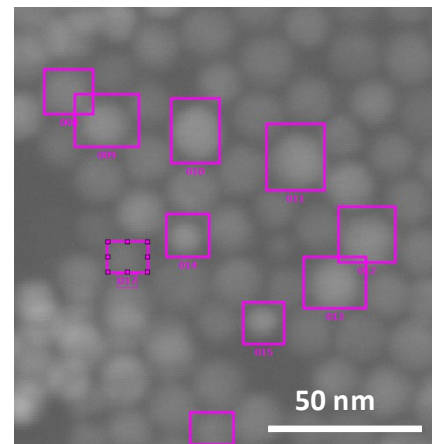


Figure S10. EDX analysis performed on isolated nanoparticles of sample CS_CoF3.

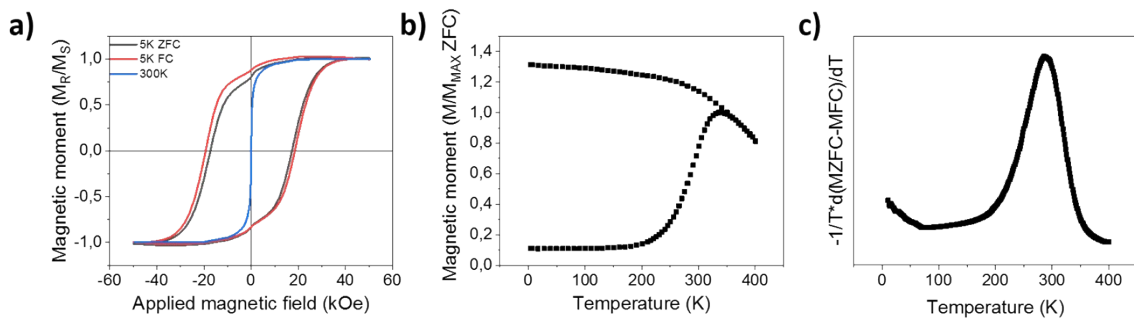


Figure S11. Magnetic properties of core-shell nanoparticles for CS_CoF3. a) ZFC and FC $M(H)$ curves recorded at 300 K and 5 K. b) ZFC and FC $M(T)$ curves. c) The blocking temperature distribution corresponding to $f(T_B) \approx -(1/T)(d(M_{ZFC}-M_{FC})/dT)$.